AIP | Journal of Applied Physics

Fractal analysis of Xylella fastidiosa biofilm formation

A. L. D. Moreau, G. S. Lorite, C. M. Rodrigues, A. A. Souza, and M. A. Cotta

Citation: J. Appl. Phys. **106**, 024702 (2009); doi: 10.1063/1.3173172

View online: http://dx.doi.org/10.1063/1.3173172

View Table of Contents: http://jap.aip.org/resource/1/JAPIAU/v106/i2

Published by the AIP Publishing LLC.

Fractal analysis of *Xylella fastidiosa* biofilm formation

A. L. D. Moreau,[1,a)] G. S. Lorite,[1] C. M. Rodrigues,[2] A. A. Souza,[2] and M. A. Cotta[1]
[1]*IFGW, DFA, UNICAMP, C.P. 6165, 13083-970 Campinas, São Paulo, Brazil*
[2]*Centro APTA Citros Sylvio Moreira/Instituto Agronômico, C.P. 04, CEP 13490-970, Cordeirópolis, São Paulo, Brazil*

(Received 5 December 2008; accepted 17 May 2009; published online 30 July 2009)

We have investigated the growth process of *Xylella fastidiosa* biofilms inoculated on a glass. The size and the distance between biofilms were analyzed by optical images; a fractal analysis was carried out using scaling concepts and atomic force microscopy images. We observed that different biofilms show similar fractal characteristics, although morphological variations can be identified for different biofilm stages. Two types of structural patterns are suggested from the observed fractal dimensions D_f. In the initial and final stages of biofilm formation, D_f is 2.73 ± 0.06 and 2.68 ± 0.06, respectively, while in the maturation stage, $D_f = 2.57 \pm 0.08$. These values suggest that the biofilm growth can be understood as an Eden model in the former case, while diffusion-limited aggregation (DLA) seems to dominate the maturation stage. Changes in the correlation length parallel to the surface were also observed; these results were correlated with the biofilm matrix formation, which can hinder nutrient diffusion and thus create conditions to drive DLA growth. © *2009 American Institute of Physics*. [DOI: 10.1063/1.3173172]

I. INTRODUCTION

Spatial patterns formed by growing systems have been extensively studied due to the large morphological variations observed with changes in the parameters controlling growth. Many systems, from thin films and crystal surfaces[1,2] to tumors[3,4] and bacterial colonies,[5–7] can exhibit complex spatial patterns during the growth process. In particular, the morphological patterns formed by biological systems such as bacteria[8–10] and fungi[11,12] colonies were shown to exhibit typical characteristics of several growth models such as Eden,[10] reaction-limited aggregation (RLA),[11] and diffusion-limited aggregation (DLA).[13,14] The Eden model assumes that a compact cluster forms through the addition of a new particle (a fungus or a bacterium formed by cellular division, for example) at any randomly chosen surface site of the cluster, without any barriers or limitations to this aggregation.[15] On the other hand, DLA models aggregation in any system where diffusion is the primary means of transport; thus particles undergoing a random walk due to Brownian motion cluster together to form aggregates. In the particular case of bacteria, cluster formation depends on nutrient diffusion by Brownian motion, which drives the growth by cellular division. Thus local gradients in the nutrient distribution can cause branch formation in the cluster[5,10,11] due to a screening effect. For biological systems, the recruitment of new cells by diffusion from the medium occurs as well; however, this event has a much lower probability than cellular division due to the low bacteria concentration in the media and it is thus generally neglected.[10]

Fractal analysis of growing surfaces is an important tool to determine the mechanisms driving morphology formation.[16] The scaling behavior and critical exponents (or fractal dimension) observed experimentally are usually compared to predictions from continuous models based on the mathematical description of the most likely surface processes; thus the main driving forces behind surface dynamics can be ascertained. The surface of bacterial colonies, in particular, can also be understood as a similar problem and modeled accordingly. Computational simulation at two and three dimensions has been carried out for bacteria and fungi growth, limited by nutrient diffusion.[5,14] The calculated fractal dimensions in those cases agree well with the Eden and DLA models. From the experimental point of view, Wakita *et al.*[10] studied the bacterial colonies in agar plates and observed that the colony growth exhibited a fractal dimension of $D_f = 1.73 \pm 0.02$, very close to that expected for the two dimensional DLA model, $D_f \sim 1.7$. When the nutrient concentration was altered, the system morphology varied as well;[10] for a high nutrient concentration, the system showed an Eden-like[5] pattern. However, when the nutrient concentration was lowered, DLA-like patterns dominated the morphology.

Some types of bacterial colonies, however, can form biofilms, which are colonies marked by the secretion of a protective and adhesive matrix, formed mainly by an extracellular polymeric substance (EPS). This kind of structure brings several advantages for the biological system; for example, it enhances the protection of cells within its volume and facilitates the communication through biochemical signals, namely, *quorum sensing*. Biofilms have been found to contain water channels that help distribute nutrients and signaling molecules. The development of biofilms also allows the cells to become drug resistant.[17–20]

One interesting system where biofilms have been studied in recent years is *Xylella fastidiosa* (*X. fastidiosa*). This bacterium is responsible for several economically important diseases in plants such as citrus, grapevine, plum, almond, peach, and coffee.[20,21] In Brazil, it is responsible for the citrus variegated chlorosis, a disease that causes annual losses

a)Electronic mail: amoreau@ifi.unicamp.br.

of more than $100 million to the citrus agroindustry.[22] *X. fastidiosa* is the first phytopathogenic bacterium for which a complete genome sequence was determined.[23] The pathogenicity of *X. fastidiosa* is a result of the biofilm formation inside the plant xylem vessels leading to blockage and consequent water stress. This pathogenicity mechanism differs from other phytopathogenic gram-negative bacteria, which depend on the type III secretion system, constituting a new way of causing disease in plants.[24] In this case, understanding the growth of such biofilms is a key issue in trying to find mechanisms to prevent their formation.

In this work, the growth processes of *X. fastidiosa* biofilm were studied since their early formation until a final stage after a period of 30 days. The bacteria were inoculated on a glass surface, without media replenishing. The distance and size of the biofilms were analyzed with optical and atomic force microscopy (AFM) images. Dynamical scaling concepts were used with AFM images in order to characterize the growth process. With this study, we suggest that the morphology and structure of *X. fastidiosa* biofilm have a direct relation to the environment nutrient concentration as well as inoculation time and EPS production.

II. METHODOLOGY

The 9a5c bacterial strain of *X. fastidiosa* subspecies *pauca*[25] was used in this study. This strain was the same as that used for genome sequencing and obtained from Institut National de La Recherche Agronomique (INRA) (Bordeaux, France). Bacterial cells are shaped as small slender rods, with sizes in the range 250–300 nm in diameter and 0.9–3.5 μm in length.[26] The bacteria were inoculated into the plant to maintain their pathogenicity state and avoid attenuation due to successive passages in axenic medium. Petioles and stems were aseptically ground in phosphate buffered saline (PBS) buffer and the suspension was spread on periwinkle wilt (PW) medium.[27] The first colonies were observed between 10 and 15 days after inoculation and such cells were used in the experiments.

In order to obtain *X. fastidiosa* biofilms we used an experimental protocol developed by Souza *et al.*[21] *X. fastidiosa* cells were incubated at 28 °C on 12 mm diameter cover glass slips immersed in PW medium in "Nunclon delta SI Multidish 24 wells" (Nunc A/S, Roskilde, Denmark). For that, five individual colonies were transferred to a microcentrifuge tube containing 1 ml of PW broth. The tubes were vortexed and the cell suspension was transferred to the wells. The biofilm of *X. fastidiosa* strain 9a5c was analyzed at 5, 10, 15, 20, and 30 days after inoculation. Three glass cover slips were analyzed for each time point. The samples were rinsed, dried, and previously coated with an ~50-nm-thick sputtered gold film.

The *X. fastidiosa* becomes a complete biofilm approximately after 15 days, when is possible to detect EPS formation around the biofilm.[21] In our samples, however, the EPS was removed during the preparation process for gold coating by sputtering. It is also possible that some biofilms detached from the substrate due to sample preparation. However, all samples were processed similarly to allow a comparative analysis.

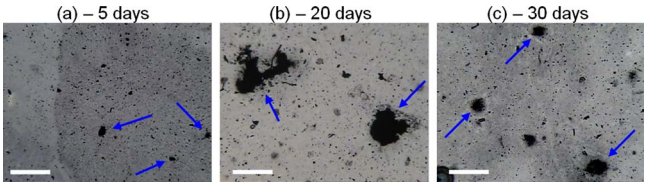

FIG. 1. (Color online) Optical microscopy images of *X. fastidiosa* biofilm with different growth time. The scale bar corresponds to 100 μm.

The samples were characterized by Normaski optical microscopy for a description of average size and distance between biofilms. We used the IMAGE J software[28] to estimate the area of the biofilms. For that we assumed circular areas and mapped its average diameter and center. For each biofilm, distances to the nearest three or four nearest neighbors were considered.

AFM analysis was carried out in air with an Agilent 5500 in noncontact mode and conical Si tips with a radius less than 10 nm and length ~20 μm, which made measurements of large *X. fastidiosa* biofilms possible.

The rms surface roughness W of the images was calculated from

$$w(L,t) = \langle (h^2(\mathbf{x},t) - \bar{h}^2)^2 \rangle_{\mathbf{x}}^{1/2}, \tag{1}$$

where L and t represent the size and growth time of the sample, respectively.

We acquired AFM images with 10×10, 20×20, and 30×30 μm^2 scan sizes in order to scan close to the center of a single biofilm and avoid edges or the substrate. The roughness dependence on the system size was studied using the box counting technique.[29] From this dependence we have used the dynamic scaling theory according to[16]

$$w(L) \sim L^{\alpha} \tag{2}$$

in order to extract the roughness exponent α. The fractal dimension was calculated from $D_f = 3 - \alpha$.[16] The correlation length ξ was extracted from W versus L curves at the crossover to the roughness saturation regime. The results shown here (and their associated error bars) express the average of four to eight images for each sample—i.e., we have analyzed different biofilms on the same sample—for the evaluation of the roughness exponent α and correlation length ξ.

The gold film roughness in the AFM images was orders of magnitude smaller than that of the biofilms, so its contribution to our analysis could be neglected.

III. EXPERIMENTAL RESULTS AND ANALYSIS

Figure 1 shows optical microscopy images of *X. fastidiosa* samples. The dark clusters indicated by arrows show typical examples of bacterial biofilms.

Table I shows the average values obtained for diameter and distance between nearest neighbor biofilms for the different samples considered in this study. Although there is a large dispersion of values due to the relatively small number of biofilms in each sample (~20), we can notice that the sample grown for 20 days presents the maximum value both

TABLE I. Average diameters and distances between biofilms evaluated from optical images.

Growth time (days)	Average diameter (μm)	Average distance (μm)
5	81 ± 52	280 ± 150
10	68 ± 25	400 ± 200
15	93 ± 53	420 ± 200
20	111 ± 49	500 ± 250
30	78 ± 26	470 ± 170

for biofilm diameter and distance between neighbors. This result indicates that, in the first stages of growth, there might be a competition process where some biofilms grow in size at the expense of the smaller ones—otherwise the distance between neighbors would not increase in size with the biofilm diameter. This process may be related to local nutrient gradients caused by the fastest growing biofilms.[5,30] However, for samples grown for periods larger than 20 days, the biofilm diameter shrinks significantly while the average distance to the neighbors shows a slight decrease. This behavior may be attributed both to local nutrient depletion in the media as well as to the detachment of bacteria from the biofilm for the nucleation at new sites on the substrate.

Figure 2 shows AFM images for samples with 5, 20, and 30 days of growth time. We can notice that all of them show a compact mass of bacteria in the background with some more compact aggregates on the top. These aggregates are usually larger for the samples with 20 days (as shown by the profiles in the bottom of Fig. 2); their shape, observed in small area scans, suggests a cluster of more vertically oriented bacteria. Associated with the larger sizes observed for these samples in optical microscopy, the aggregates could be related to a branchlike formation on the surface, caused either by nutrient competition[5,10,11,30] or by bacteria trying to detach from the biofilm. Indeed, for samples with 30 days of growth time, the aggregates are smaller and the morphology shows a more homogeneous bacteria coverage.

Figures 3(a) and 3(b) show 30×30 μm^2 typical AFM images of two different *X. fastidiosa* biofilms on the same sample, with 10 day growth time. These images were acquired on the central regions of the biofilms to avoid edges where the substrate might be exposed as well. Figure 3(c) shows the roughness behavior with system size (W versus L curves) for images in Figs. 3(a) and 3(b), with the respective fittings to identify the values for the roughness exponent (α) and correlation length (ξ). It is clear that, even for these small scans, roughness saturation occurs. From the fittings, we can observe, for each curve, two values of α and ξ, which are also shown in the figure. The first set of values, α_1 and ξ_1, is associated with the surface structures with a smaller length scale. They should represent the individual bacterium, since ξ_1 has the same order of magnitude of *X. fastidiosa* average size, ~ 1 μm.[31] The second set of values (α_2 and ξ_2), however, must also carry information on the conformational characteristics of the biofilm.

We get a very good agreement for α and ξ values obtained for both images (differences up to 5%), indicating that different biofilms show similar behavior when grown on the same sample; the same analysis was extended to several biofilms on the different samples, providing similar results. The offset between the two curves provides slightly different roughness saturation levels. However, this difference, ~ 350 nm, is of the order of the average bacterium diameter (~ 300 nm).[26]

The statistical similarity observed for biofilms on the

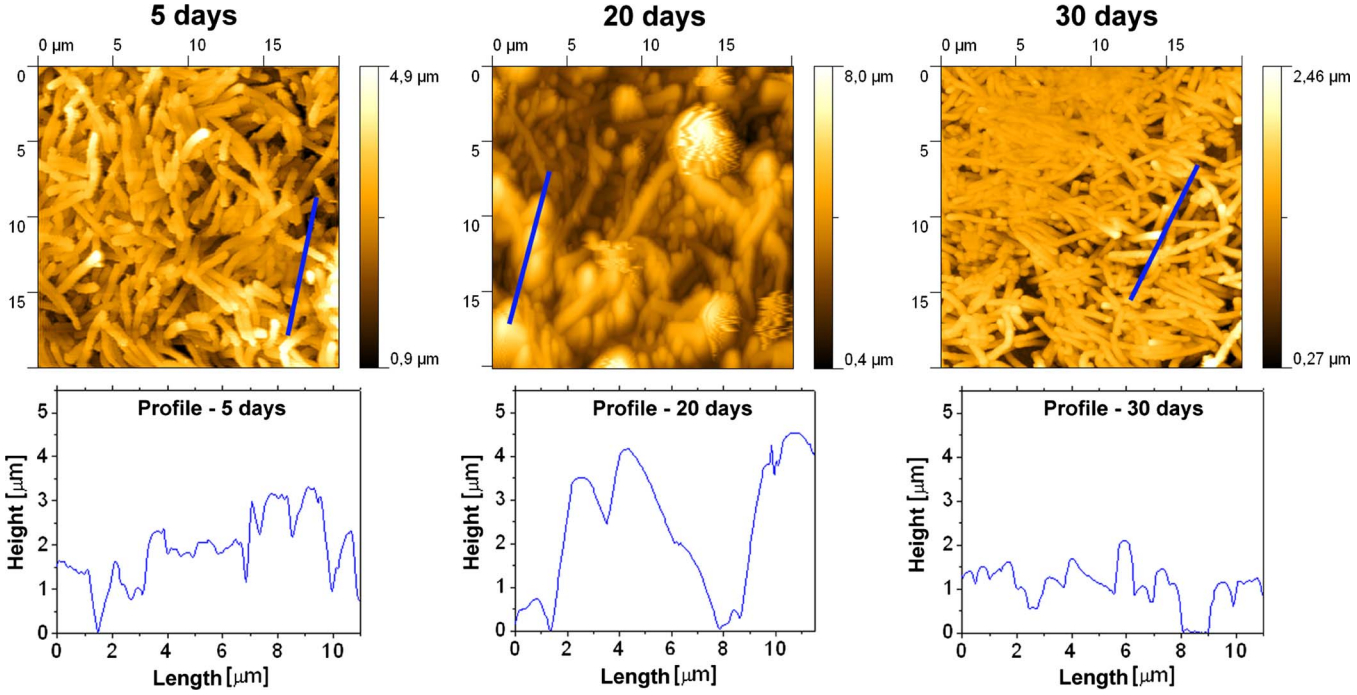

FIG. 2. (Color online) Typical AFM images of *X. fastidiosa* biofilms for 5, 10, and 30 days. The bottom plots show the cross section profiles corresponding to the blue lines in the AFM images.

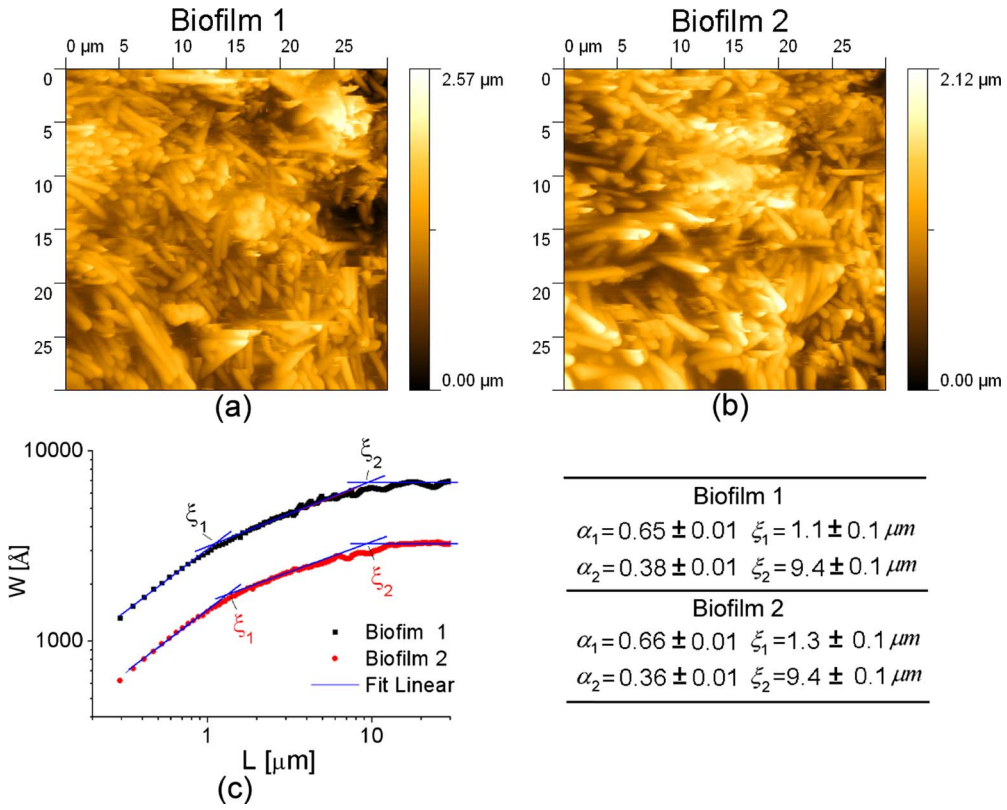

FIG. 3. (Color online) [(a) and (b)] AFM images for two different biofilms of *X. fastidiosa* on the same sample (with 10 days). (c) Roughness vs size (*W vs L*) plots of AFM images in (a) and (b). Roughness exponents and correlation lengths for the curves in (c) are also shown. The error bars for both exponents are provided from fitting the curves in (c).

same sample—as shown in Fig. 3—provides a basis for a fractal analysis of the AFM images for biofilms in different stages. Figure 4 shows the dependence of fractal dimension D_f and correlation length (ξ) on the growth time, for the different samples considered in this work. In this figure the values shown are obtained from averaging over several colonies for each sample. Figure 4(a) shows that D_f varies between 2.5 and 2.8, with a trend to smaller values as the growth time reaches 20 days. For biofilms with a smaller growth time, 5–15 days of inoculation,[21] the average fractal dimension values observed, $D_f = 2.73 \pm 0.06 \sim 2.66 \pm 0.03$, are closer to that expected from three-dimensional Eden-like models,[15] $D_f \sim 2.7$. On the other hand, for the more mature biofilms (growth time of 20 days), the fractal dimension drops to $D_f = 2.57 \pm 0.08$, a value closer to that expected from DLA-like models,[13,31,32] $D_f \sim 2.5$. After this point, for the sample with 30 days, D_f increases to 2.68 ± 0.06.

Matsushita and Fujikawa[30] suggested that biofilm growth is ruled primarily by nutrient diffusion; the contribution of bacteria diffusion and recruitment from planktonic state should be minimum.[5,10,30] When the nutrient concentration is high, cell division can occur randomly on the biofilm surface. If we consider our data from optical microscopy and AFM analysis, the biofilm formation for smaller growth times should be occurring under richer media conditions, which do not hinder bacteria growth. These conditions may be well described by the Eden model. However, the larger biofilms observed at 20 days exhibited a DLA-like growth

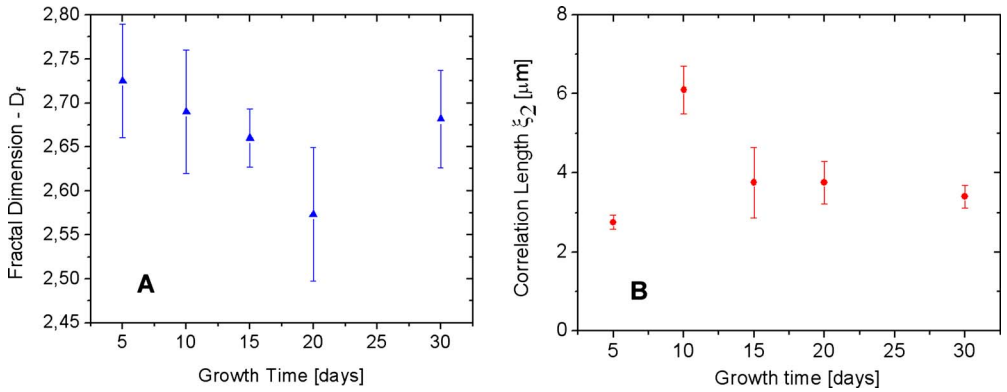

FIG. 4. (Color online) (a) Fractal dimension and (b) correlation length dependence on growth time of *X. fastidiosa* biofilms. The error bars reflect the average on different colonies and image scan sizes for the same sample.

fractal dimension. We can assume that the nutrient diffusion should be slowed down due to both the larger biofilm volume and the more complex architecture in this case; a well established EPS matrix should provide an extra barrier for the nutrients' diffusion. In that case, screening effects and shadowing at certain regions of the cluster, predicted from DLA models, could be associated with the larger aggregates observed in AFM images (Fig. 2).

At 30 days, D_f values grow up to 2.68 ± 0.06. These values indicate that the system returns to an Eden growth model. The decrease in size observed by optical microscopy plus the smaller areas/volumes confirmed by AFM indicate that these biofilms are in the degradation process, where the nutrient concentration should no longer play a major role.

Gerlee and Anderson[5] studied theoretically the growth dynamics and spatial patterns of bacteria colonies under nutrient limited conditions. By observing that the local growth of the colony is proportional to the flux of the nutrient, Gerlee and Anderson[5] derived an approximate dispersion relation for the growth of the colony interface. This relation shows that the stability of the growth depends on how far the nutrient penetrates into the colony. For low nutrient consumption rates the penetration distance is large; under this condition, growth is stable and the colony acquires a compact form. On the other hand, for high consumption rates, the penetration distance is small, which leads to unstable branched growth. We can relate this result to the experimental behavior observed in our system. The optical images were used to analyze the perimeter of the biofilm, while the AFM images allowed the study of the biofilm's innermost regions, as mentioned in Sec. II. The optical images show that, for the sample with 20 days, most biofilms presented an irregular shape, as observed in Fig. 1(b). This irregular shape can be viewed—at this magnification scale—as a branch pattern. For samples with 5, 10, and 30 days [as seen in Figs. 1(a) and 1(c)], most biofilms presented a circular perimeter, suggesting a more compact pattern. Furthermore, the 15 day sample presents both irregularly and regularly shaped biofilms, suggesting that they are at an intermediate phase. These results correlate very well with the AFM scaling analysis, since circular shapes are expected from Eden models, while the branched pattern is associated with DLA. We can thus suggest that, in our case, for samples with smaller growth times (until ~ 15 days), where the biofilm is not yet completely formed, large penetration of nutrients is allowed and a compact, circular shape for the colony is achieved, as expected from Eden models. When the biofilm reaches the maturation stage (~ 20 days), both the larger number of bacteria and the EPS diffusion barrier hinder the penetration of the nutrients in the biofilm, thus leading to branch formation, which can be associated with a DLA pattern. After this stage, the biofilm starts to degrade, and the rate of nutrients' consumption drops. Although the nutrient concentration in the medium should be already low in this phase, the diminished number of bacteria could compensate this effect, returning the biofilm to a more compact shape, which is a characteristic of an Eden pattern.

The growth process usually shows lateral correlations along the surface, which implies that different sites on the surface are not completely independent—but instead depend on the heights of the neighboring sites as well. These correlations are expressed by the data in Fig. 4(b), which shows the variation of the correlation length with growth time; a value between 2.8 and 4 m is observed for four samples—except for a larger ξ value at 10 days. The former values suggest that the lateral correlations are mainly associated with the nearest neighbors on the surface. This result agrees with the scenario where the biofilm growth is mainly driven by cell division and not by capture from planktonic cells.

Souza *et al.*[21] described that *X. fastidiosa* colonies transform into biofilms, and consequently start to produce the EPS matrix, after 10 days of inoculation. The biofilm is completely formed around 15 days. We could associate this fact with the large ξ value for 10 days (~ 6 μm) since EPS production could change lateral correlations within the growing surface structure without drastically altering its morphology (as observed from AFM images). The lower ξ values for samples with more than 10 days can be interpreted as the stabilization of EPS production and biofilm formation.

IV. CONCLUSIONS

AFM and optical microscopy images were used to observe the formation and growth of *X. fastidiosa* biofilms through the characterization of their morphology, size, and nearest-neighbor distance with growth time. The observed changes could be associated with two main factors: nutrient concentration and EPS formation. Eden and DLA models can be used to explain the observed scaling properties for the biofilms. The onset of EPS formation at 10 days is associated with a decrease in the fractal dimension until 20 days (when biofilm matures), as well as an increase in the lateral correlation length, suggesting a DLA-like growth.

ACKNOWLEDGMENTS

This work was financially supported by FAPESP (Grant Nos. 04/14576-2 and 04/09132-8), CNPq, and CAPES. A.A.S. and M.A.C. are recipients of CNPq research fellowships.

[1] G. S. Lorite, V. R. Coluci, M. I. N. da Silva, S. N. Deziderio, C. F. O. Graeff, D. S. Galvão, and M. A. Cotta, J. Appl. Phys. **99**, 113511 (2006).
[2] J. R. R. Bortoleto, M. A. Cotta, and M. M. G. de Carvalho, Surf. Sci. **515**, 117 (2002).
[3] E. Khain and L. M. Sander, Phys. Rev. Lett. **96**, 188103 (2006).
[4] A. Bru, J. M. Pastor, I. Fernaud, I. Bru, S. Melle, and C. Berenguer, Phys. Rev. Lett. **81**, 4008 (1998).
[5] P. Gerlee and A. R. A. Anderson, Phys. Rev. E **75**, 051911 (2007).
[6] M. Obert, P. Pfeifer, and M. Sernetz, J. Bacteriol. **172**, 1180 (1990).
[7] C. Kampichler, J. Rolschewski, D. P. Donnelly, and L. Boddy, Soil Biol. Biochem. **36**, 591 (2004).
[8] T. Vicsek, M. Cserzo, and V. K. Horvath, Physica A **167**, 315 (1990).
[9] H. Fujikawa and M. Matsushita, J. Phys. Soc. Jpn. **60**, 88 (1991).
[10] J. Wakita, K. Komatsu, A. Nakahara, T. Matsuyama, and M. Matsushita, J. Phys. Soc. Jpn. **63**, 1205 (1994).
[11] J. M. Lopez and H. J. Jensen, Phys. Rev. E **65**, 021903 (2002).
[12] T. Sams, K. Sneppen, M. H. Jensen, C. Ellegaard, B. E. Christensen, and U. Thrane, Phys. Rev. Lett. **79**, 313 (1997).
[13] T. A. Witten and L. M. Sander, Phys. Rev. Lett. **47**, 1400 (1981).
[14] P. Meakin, Phys. Rev. A **27**, 1495 (1983).
[15] R. Jullien and R. Botet, J. Phys. A **18**, 2279 (1985).
[16] A. L. Barabási and H. E. Stanley, *Fractal Concepts in Surface Growth* (Cambridge University Press, Cambridge, 1995).

[17]T. F. C. Mah and G. A. O'Toole, Trends Microbiol. **9**, 34 (2001).
[18]H. M. Lappin-Scott, J. W. Costerton, and J. Lynch, *Microbial Biofilms* (Cambridge University, Cambridge, 2003).
[19]L. L. R. Marques, H. Ceri, G. P. Manfio, D. M. Reid, and M. E. Olson, Plant Dis. **86**, 633 (2002).
[20]E. Alves, "Xylella fastidiosa—Adhesion and colonization in xylem vessels of sweet orange, coffee, plum and tobacco, and insect vectors and formation of biofilm on polystyrene surface," Ph.D. thesis, Piracicaba, Universidade de São Paulo (USP), Brazil, 2003.
[21]A. A. Souza, M. A. Takita, H. D. Coletta, C. Caldana, G. M. Yanai, N. H. Muto, R. C. de Oliveira, L. R. Nunes, and M. A. Machado, FEMS Microbiol. Lett. **237**, 341 (2004).
[22]W. B. Fernandes, Jr., "Analyses of the world processed orange industry," Ph.D. thesis, University of Florida, Gainesville, FL, 2003.
[23]A. J. G. Simpson *et al.*, Nature (London) **406**, 151 (2000).
[24]A. A. Souza, M. A. Takita, E. O. Pereira, H. D. Coletta-Filho, and M. A. Machado, Curr. Microbiol. **50**, 223 (2005).
[25]N. W. Schaad, E. Postnikova, G. Lacy, M. B. Fatmi, and C. J. Chang, Syst. Appl. Microbiol. **27**, 290 (2004).
[26]J. M. Wells, B. C. Raju, H. Y. Hung, W. G. Weisburg, L. Mandelcopaul, and D. J. Brenner, Int. J. Syst. Bacteriol. **37**, 136 (1987).
[27]M. J. Davis, W. J. French, and N. W. Schaad, Phytopathology **71**, 869 (1981).
[28]IMAGE J, http://rsb.info.nih.gov/ij/.
[29]M. V. H. Rao, B. K. Mathur, and K. L. Chopra, Appl. Phys. Lett. **65**, 124 (1994).
[30]M. Matsushita and H. Fujikawa, Physica A **168**, 498 (1990).
[31]H. E. Stanley, A. Coniglio, S. Havlin, J. Lee, S. Schwarzer, and M. Wolfd, Physica A **205**, 254 (1994).
[32]H. E. Stanley, A. S. Havlin, J. Lee, E. Roman, and S. Schwarzer, Physica A **168**, 23 (1990).